

1 ***Establishing wonder oil,***
2 ***Solanesol, as a novel inhibitor for***
3 ***Focal Adhesive Kinase by in silico***
4 ***strategies***

5
6
7
8
9
10
11
12
13
14
15
16
17
18
19
20
21
22

23

24 Betty Daneial¹, Devashish Das², Jacob Paul V.J¹, Guruprasad R^{3*}

25 *1. Department St Joseph's college, Bangalore, India.*

26 *2. Scientist, Educept, New Delhi, India*

27 *3. Scientific Director, Durga Femto Technologies and Research (DFTR), #22, 4th main, 4th cross,*

28 *Chamrajpet, Bangalore-560018, India, drgp@dftr.org, Mo.+91-9880293053, Corresponding*

29 *Author*

30

31 **Establishing wonder oil, Solanesol, as a novel inhibitor for Focal Adhesive**
32 **Kinase by *in silico* strategies**

33 Focal adhesion kinase (FAK) plays a primary role in regulating the activity of many
34 signaling molecules. Increased FAK expression has been implicated in a series of cellular
35 processes, including cell migration and survival. Inhibiting the activity of FAK for cancer
36 therapy is currently under investigation. Hence, FAK and its inhibitors has been the subject
37 of intensive research. To understand the structural factors affecting inhibitory potency,
38 kinetic analysis, molecular docking and molecular dynamics simulation were studied in
39 this project. Though, Solanesol was found have inhibitory activities towards FAK, no *in*
40 *silico* tests were ever done on the same.

41 Due to high flexibility of Solanesol (Rotatable bonds = 25), it is difficult to analyze using
42 normal docking protocols. This paper introduces a novel method to dock and analyze
43 molecules with high flexibility based on weighed contact based scoring method. This
44 method uses blind docking technique, which was developed for protein peptide docking
45 method, to generate conformations which were used to calculate contact based weights of
46 residues. This method reveals the possible binding site for the small molecule. An
47 exhaustive docking search on the acquired area reveals the docked confirmation of the
48 compound. The final docked conformation was subjected to molecular dynamics to
49 understand of binding stability. This study is in a good agreement with experimental results
50 which shows Solanesol binds at ATP binding site and inhibit the phosphorylation of Focal
51 Adhesion Kinase.

52 Keywords: FAK; Solanesol; blind docking; contact scoring; mmpbsa;

53

54

55

56

57

58 **Background**

59 *Focal Adhesion Kinase*

60 Among the 10 hallmarks of cancer, “Tissue Invasion and Metastasis”, is the most devastating
61 one, as it allows the oncogenic cells to migrate to new areas in the body with more open space
62 and more nutrients. It significantly reduces survival rates and prognosis for patients. The loss of
63 cellular adhesion to the extracellular matrix regulation can lead to increased cellular
64 proliferation, decreased cell death, and altered cellular differentiation status and cellular
65 migratory capacity (Hanahan & Weinberg, 2000; Hanahan & Weinberg, 2011; Lazebnik, 2010;
66 van Nimwegen & van de Water, 2007).

67 The FAK4 family kinases, including Focal Adhesion Kinase (FAK), regulate cell adhesion,
68 migration, and proliferation in a variety of cell types. Focal adhesions are heterodimeric-
69 transmembrane integrin receptors located within sites of close opposition to the underlying
70 matrix which mediate adhesion of cells to extracellular matrix. TYR397 position FAK
71 phosphorylation simulated by Integrin engagement and clustering creates high affinity binding
72 site for SRC and SRC family kinases. In turn, FAK-SRC complex phosphorylates many
73 components of focal adhesion, which result in changes in initiation of signaling cascades and
74 adhesion dynamics. Other than the FAK catalytic activity, FAK additionally functions as a
75 scaffold to organize signaling and structural proteins within focal adhesions (Cohen & Guan,
76 2005; Guan, 1997).

77 Alteration in FAK expression not only have been associated with tumorigenesis and increased
78 metastatic potential, it is also reported to cause multiple cancers, including colon, breast, thyroid,
79 prostate, cervical, ovarian, head and neck, oral, liver, stomach, sarcoma, glioblastoma, and

80 melanoma (Guan, 1997).

81

82 *Solanesol*

83 Solanesol is a polyisoprenoid alcohols or polyprenols, found mainly accumulates in solanaceous
84 crops, including tobacco, tomato, potato, eggplant, and pepper plants. In industries, Solanesol is
85 extracted commercially from its richest source, tobacco plant. Commercially, Solanesol is widely
86 used as an intermediate for the synthesis of ubiquinone drugs, such as coenzyme Q10 and
87 vitamin K2 as well as Vitamin K and Vitamin E. It is known to possess activities like antibacterial,
88 antifungal, antiviral, anticancer, anti-inflammatory, and anti-ulcer activities, and its derivatives
89 also have anti-oxidant and anti-tumor activities, in addition to other bioactivities (Yan et al.,
90 2015; Srivastava et al, 2009; Suzuki, Tomida & Nishimura, 1990; Tomida & Suzuki, 1990;
91 Zhao, Zu, Li, & Tian, 2007; Severson, Ellington, Schlotzhauer, Arrendale, & Schepartz, 1977).
92 Derivatives of Solanesol, (S)-2,3-dihydropolyprenyl, monophosphate, and agents for inhibiting
93 the metastasis of cancers (Okamoto, Tsuji, & Yamazaki, 1994).

94 *Objective*

95 The main aim of this paper is to establish Solanesol as a Focal adhesion kinase inhibitor by the
96 means of *in silico* methods. Though Solanesol is used as a bioactive agent in industries for decades,
97 due to its highly flexible nature, there is no successful *in silico* protein binding and simulation
98 data available online till date.

99 Solanesol has 25 rotatable bonds which makes it very difficult to dock directly to the protein
100 structure by conventional methods. Although there are various methods for prediction of binding

101 site in FAK, the flexible nature of Solanesol as well as the size of the compound makes it
102 difficult to fit the active site. For the purpose of predicting the actual binding site, blind docking
103 method can be used. Blind docking method was introduced for the purpose of docking peptide
104 molecules to the protein molecule but is a tested method for binding of small molecules when
105 binding site is unknown (Hetényi & van der Spoel, 2006).

106 Method of blind docking comprise of locking of ligand molecule's all the torsions, for the
107 purpose of reducing calculation time, and then docking on the complete protein surface. Then the
108 best cavity or binding pocket is selected, based on the clustering of highest binding affinity
109 conformations (Hetényi & van der Spoel, 2006; Hetényi & van der Spoel, 2002).

110 In this paper we propose a method of binding of highly flexible compound to protein targets with
111 using an enhanced contact based scoring method. This method scores the residues rather than the
112 conformations. The higher scored residues were then used for more "focused" docking on those
113 residue region.

114 **Materials and methods**

115 *Protein selection and preparation*

116 The crystallographic co-ordinates for Focal adhesion kinase (PDB ID: 4Q9S) (George et al,
117 2014) were retrieved from the Protein Data Bank (PDB). Prior to docking, protein structures
118 were prepared by removing water molecules using UCSF Chimera software (Pettersen et al,
119 2004). Following which, bond orders were assigned, and hydrogen atoms were added to the
120 crystal structures.

121 ***Ligand preparation***

122 Solanesol exist in both cis and trans states, for this experiment we considered only trans as it is
123 only found in natural sources (Roe, Oldfield, Geach, & Baxter, 2013). The structure of Solanesol
124 was obtained from PubChem compound (CID 5477212) (Kim et al, 2015; NCBI 2016). Gaussian
125 09 program (Frisch et al, 2009) was used to obtain the optimum geometry of the structures using
126 the density function theory at the B3LYP/6-31G (d,p) level.

127 ***Molecular docking***

128 All the molecular docking studies of Solanesol to FAK were performed using Autodock 4.2
129 (Morris et al, 2009). Autodock uses a semi-empirical free energy force field to evaluate binding
130 conformations of ligand while docking. The AutoDockTools (Morris et al, 2009) was used for
131 preparing protein and ligand parameters files.

132

133 ***Binding site analysis:***

134 Solanesol is a 45 carbon chain with 26 rotatable bonds. As it is extremely flexible it is hard to
135 determine the bind mode of it with the protein. The commonly used protocol for determination of
136 binding pocket is “Blind docking”, which was initially developed for to determining peptide
137 docking with protein (Hetényi & van der Spoel, 2006; Hetényi & van der Spoel, 2002). In this
138 method the constrained ligand (or peptide) is docked with the whole protein surface. The place
139 where it forms a cluster with higher energy determines the binding site. Then these sites were
140 used for “refined docking” where the lowest binding modes for each of these places (in case if
141 there are more than one) where determined by molecular mechanics and molecular dynamics
142 studies.

143 For calculating the possible area of interaction or binding site of a highly flexible ligand we
144 enhanced blind docking using Ligand Contact Based Scoring function for Residues (LCBSR).
145 This is an atomic contact\clash based scoring method, in which the residues are scored based on
146 the higher favorable interactions and probability of formation of a hydrogen bond. As it doesn't
147 depend on the clustering or solely on binding energy, it statistically enhances the probability of
148 finding the possible binding site.

149 It can be represented as,

$$150 \quad \text{LCBSR} = \log(N_{Co} - N_{Cl}) - \log(N_H/C_{Cl}) \quad (1)$$

151 Where, ligand contact based scoring of residue (LCBSR) is calculated using “Number of
152 Contacts” (N_{Co}) which is the number of occurrences where atoms of residue (r) are in contact
153 with any atom of the ligand in all the conformations. “Number of Clashes” (N_{Cl}) is the number
154 of occurrences when atoms of residue (r) are in clashes or unfavorably overlapped with any atom
155 of the ligand in all the conformations. “Number of Hydrogen Bonds” (N_H) is the number of
156 occurrences when atoms of residue (r) are forming a hydrogen bond with any atom of the ligand
157 in all the conformations. “Number of Clashes” (C_{Cl}) is the number of conformers where residue
158 (r) is in an unfavorable overlap with any atom of the ligand.

159 The “Contact” here is defined as the instance when the difference between the distance of two
160 atoms and the sum of their van der Waal radii is 0.4 Å or more or, in other words, the distance is
161 greater than the sum of van der Waal radii (Eq 1) of two atoms. Whereas “Clash” is defined as
162 the condition where the van der Waal radii of two atoms unfavourably overlaps each other and
163 the distance is lower than the sum of radii (Eq 2) of the two atoms. This can be represented as:

164
$$\Sigma r_{VDW}(i,j) - D_{ij} \geq -0.4 \quad (2)$$

165
$$\Sigma r_{VDW}(i,j) - D_{ij} \geq 1.0 \quad (3)$$

166 Where, $\Sigma r_{VDW}(i,j)$ is the sum of van der Waal radii of interacting atoms of ligand (i) and residue
167 (j) and D_{ij} is the distance between interacting atoms of ligand (i) and residue (j). A Higher value
168 of LCBSR of any residue implies the residue may be a part of the binding pocket for the ligand
169 and, if it is capable, it may also form a hydrogen bond with the ligand. Lesser score implies a
170 lower interaction or high chances of unfavorable clashes or low chances of forming a hydrogen
171 bond.

172 **Experimental design:**

173 *Blind docking*

174 For this experiment, Solanesol was docked a total of 3 times (Table 1) with “Blind Docking”
175 protocol. For getting an unbiased result, all the rotatable bonds were kept unconstrained for all
176 the experiments. The protein was covered using a $126 \times 126 \times 126$ grid box with protein centre
177 as grid centre. For experiment ligand starting position was changed.

178 The docking resultant file from Autodock was then converted into multiple PDB files using
179 Autodock scripts. All the contacts and clashes, as well as hydrogen bonds between the
180 conformation and protein, were calculated using UCSF Chimera tool.

181 Considering all the conformers may lead to false positives, thus conformers were separated in
182 three criteria:

183 (1) Binding energy less than -2.0 kcal/mol

184 (2) Binding energy less than -3.0 kcal/mol

185 (3) Binding energy less than -4.0 kcal/mol.

186 Provided -4.0 is roughly half the average of the binding energy (Average B.E = -7.10 kCal/mol)
187 of all the three experiments, ensuring only conformations with low B.E were considered. The
188 resultant values from each of these three were added to corresponding residues. This way the
189 residues interacting more with the conformations of better binding energy will have a better
190 score.

191 For getting a statistically significant result, all the scores of the residues from all the three
192 experiments were added to get the final score of each residue. Only those residues which
193 appeared in more than 2 experiments were considered.

194 ***Refined docking***

195 A binding site was formed using residues with a higher LCBSR score (percentile = 0.50). This
196 binding site was then used for refined docking using Autodock. The experiment was done twice
197 with (1) relaxed parameters, GA maximum energy evaluations 2.5×10^6 , for 200 GA runs (2)
198 exhaustive parameters, GA maximum energy evaluations 3.5×10^7 , for 200 GA runs.

199 ***Knowledge-based rescoring***

200 All conformations were rescored using DSX, Drug Score eXtended, (Neudert & Klebe, 2011),
201 knowledge-based rescoring based on the DrugScore formalism, to estimate the affinity of
202 conformation for FAK. The best conformations were selected based on the rescored values. The
203 best conformation bound complex of FAK was further used for molecular dynamics simulation
204 studies.

205 ***Molecular dynamics***

206 Molecular dynamics simulations for FAK protein as well as Solanesol bound FAK were
207 performed using the GROMACS (Groningen Machine for Chemical Simulations) 4.6 (Hess,
208 Kutzner, Van Der Spoel, & Lindahl, 2008) software with GROMOS96 (53a6) force field.
209 PRODRG (Van Aalten et al, 1996) server was used to generate topology files for Solanesol.
210 Charges were kept full and no energy minimization was done using PRODRG.

211 The complex was solvated in a dodecahedron box with SPC model water model
212 molecules and periodic boundary conditions were used. One negatively charged chlorine ion (Cl-
213) was added to the system for maintaining the system's neutrality.

214 The Lincs and Shake algorithm (Hess, Bekker, Berendsen, & Fraaije, 1997) were used
215 for constraining bond length and fixing all bonds containing hydrogen atoms respectively.

216 For electrostatic calculations, Particle Mesh Ewald (PME) (Darden, York, & Pedersen,
217 1993) method was used, with a coulomb cutoff of 1.2nm, Fourier spacing of 0.16 nm and an
218 interpolation of order 4. Energy minimization of the system was carried out using steepest
219 descent algorithm with a tolerance value of 1000 kJ mol⁻¹nm⁻¹. After energy minimization,
220 NVT and NPT equilibrations were done on the system until it reached the room temperature and
221 water density. Production MD was performed for 20 ns time duration for both the simulations.

222 ***Molecular dynamics trajectories analysis***

223 Root mean square deviation (RMSD) and root mean square fluctuations (RMSF) of FAK
224 backbone were calculated using “g_rms” and “g_rmsf” utility commands, respectively. A
225 spherical probe of radius 1.4 Å across the protein surface was used for calculating solvent-
226 accessible surface area (SASA) by "g_sasa" tool of Gromacs. Hydrogen bonds between

227 Solanesol and FAK were calculated using "g_hbond" tool with proton donor and acceptor
228 distance ≤ 3.5 Å and the angle between acceptor-donor-hydrogen ≤ 30.0 degrees.

229 *Binding free energy calculations*

230 Molecular mechanics Poisson-Boltzmann surface area (MMPBSA) (Massova &
231 Kollman, 2000) approach was to estimate the binding free energy of protein-ligand interaction.
232 For this purpose, "g_mmpbsa" (Kumari, Kumar, & Lynn, 2014) tool was used. The tool
233 calculates the molecular mechanics potential energy and the free energy of solvation and
234 excludes the entropy calculations. MM-PBSA calculations were performed using 1000
235 snapshots taken from last 5 ns of trajectories of the complex system.

236 **Result & Conclusion**

237 *Docking Analysis:*

238 *Blinding docking and LBCSR Score:*

239 Solanesol was docked against FAK structure (PDB id: 4Q9S) using Autodock4.2
240 three times (as mentioned in materials & methods). For all the three times, a grid of size $126 \times$
241 126×126 with 0.375Å [Figure 1] spacing was created with protein center (Centre coordinates =
242 9.7, 0.16, 15.1) as the grid center, as per the normal "blind docking" protocol. Dielectric constant
243 value was kept default.

244 Solanesol shows very small cluster with insignificant binding affinity towards FAK when
245 docked "blindly" [Table 1]. Though, the structure show quite high binding affinity towards the
246 kinase but the conformations with higher binding energy fails to form any significant cluster.

247 From all the generated conformations of Solanesol which were having binding energy
248 lower than -4.0 kCal/mol, all the favorable and unfavorable overlaps of the atoms were calculated

249 using “FindClash” tool of UCSF Chimera. Chimera tool, “FindHbond” was also used to find the
250 hydrogen bonds between the ligand and residue atoms. The default values were kept for all the
251 calculation in Chimera.

252 An in-house python script was used to calculate the number of “Clashes”, “Contacts” and
253 “Hbonds” between all the conformations and residues as well as individual scores. The scores
254 from all the three experiments were added to give a final score for each residue [Table 2].

255 Based on the LBCSR score calculated for all three experiments, the scores for all the
256 residues were plotted as graph (Fig 3) as well as plotted as false colour on the 3D structure of the
257 protein (Fig 2). From the LBCSR score it can be inferred that the ligand shows a high affinity
258 towards the region with Asp564, Asn551, Arg550, Leu553 and Ile428, respectively.

259 *Refined docking:*

260 All the residues with more than LBCSR score was considered for the active site
261 prediction. A total of 77 residues were found to be above and incidentally which also forms the
262 ATP binding site and the catalytic loop (546-551) and formed between the N and C lobe [1].

263 Centre of geometry (Coordinates = 10.8, 1.0, 15.0) of these 77 residues were considered
264 for the centre of the binding pocket of Solanesol. A grid of size $60 \times 62 \times 68$ was considered to
265 exactly fit all the 77 residues. Autodock4.2 was again used for docking of Solanesol with FAK
266 with this grid setting for two more times, first time with default setting for 200 conformations
267 and later docked with exhaustive setting for the same number of conformations.

268 All 400 conformations were rescored using DSX online server with CSD settings. (Table 3)

269 ***Analysis of Final Docked structure:***

270 The hydroxyl end of Solanesol binds to the binding site of ATP and interacts with Ile428,
271 Val436, Ala452, Lys454 and Leu501. These residues which forms the binding pocket for ATP,
272 forms Alkyl-Pi hydrophobic interactions with the double bonds of the ligand. Whereas, the
273 isobutyl end of the ligand, gets attached with the Catalytic loop and α C helix. The ligand
274 interacts with Phe542, Arg545, Arg550 (Catalytic loop) and Phe478 (α C helix terminal) with
275 Alkyl and Sigma-Pi interactions. Pro585, Ile586 near the ATP active site also forms similar
276 hydrophobic interactions with the ligand. Oxygen of Solanesol forms a very conventional H-
277 bond with OE1 of Gln438 which is very near to G-Loop and ATP binding site.[30]

278 These 12 hydrophobic interactions of 11 residues with Solanesol stabilize the ligand at
279 the middle of N and C lobe of FAK. As the ligand share interacting residues with both the side it
280 may be act as a better inhibitor for FAK. This structure was used for molecular dynamics studies.

281 ***Analysis of Molecular Dynamics***

282 For the measuring the stability, the deviation in the backbone of the protein has been
283 measured relative to time [Fig 5]. After an initial instability, the backbone changes its shapes
284 linearly with a linear slope increase in RMSD between 4.5ns to 7.7ns after again a short
285 destabilization the system vaguely equilibrates from 9.4ns to 14.2ns. It takes the system almost
286 15ns to equilibrate, after which the system maintains its position and shape. [Fig 5]

287 Comparison of the RMSD of both the trajectories from the minimized structures shows,
288 Solanesol bound FAK backbone show more stability than that of independent FAK backbone.
289 RMSF (Root mean Square Fluctuation) of Solanesol bound FAK exhibits less fluctuation at the
290 places where Solanesol is bound [Fig 6].

291 Total solvent accessible surface area (SASA) was checked by `g_sas` tool of Gromacs for
292 analyzing the change in surface area with respect to time. It show a quite negative correlation
293 with the RMSD suggesting the better binding of the ligand leads to a lower surface area of the
294 protein thus closing the active site for any further contact. It remains stable for the wider part of
295 6ns -18ns range after which the backbone gets stabilized and may also affect the surface area.

296

297 *MM-PBSA Calculation*

298 Binding site residues for Solanesol were selected by taking 3.5Å radius from Solanesol.

299 Molecular mechanics Poisson–Boltzmann surface area (MM-PBSA) was calculated for the last 5

300 ns with 20 ps steps for the binding site residues versus Solanesol using `g_mmpbsa` tool.

301 Per residue analysis of the result was done and plotted using the script provided. This analysis

302 suggests that, Ile428, Gly431, Val436, Val484, Met499, Cys502 and Leu553 interacts most

303 favorably with the ligand. Interestingly these all residues are part of ATP binding pocket of

304 FAK. Gly431 is a part of the G-loop which helps in the phosphorylation of the protein also

305 interacts favorably along with Leu584 which is part of the activation loop.

306 MM-PBSA based binding affinity ($\Delta\Delta G$) was calculated using the `g_mmpbsa` provided script.

$$307 \quad \Delta\Delta G_{BE} = \Delta G_{Complex} - (\Delta G_{Receptor} + \Delta G_{Ligand}) \quad (4)$$

$$308 \quad \Delta G = \Delta E_{MM} + \Delta G_{Sol} - T\Delta S \quad (5)$$

$$309 \quad \Delta E_{MM} = \Delta E_{int} + \Delta E_{ele} + \Delta E_{vdw} \quad (6)$$

$$310 \quad \Delta G_{Sol} = \Delta G_{PB} + \Delta G_{SA} \quad (7)$$

311 ΔE_{MM} , ΔG_{Sol} and $T\Delta S$ represent the molecular mechanics component in the gas phase,
312 stabilization energy due to solvation, and a vibrational entropy term, respectively. ΔE_{MM} is the
313 summation of ΔE_{int} , ΔE_{col} , and ΔE_{vdw} , which are the internal, coulomb, and van der Waals
314 interaction terms, respectively. ΔG_{sol} is the solvation energy and it is divided into an electrostatic
315 solvation free energy (G_{PB}) and a non-polar solvation free energy (G_{SA}).

316 A very low $\Delta\Delta G$, of -113.85 kJ/Mol, (Table 4) proves Solanesol have a very high binding
317 affinity towards the FAK structure. The change in binding energy with time was also plotted.
318 [Fig 7], It shows that the ligand gets stabilized with a very high binding affinity after 17ns of
319 simulation.

320

321 **Conclusion**

322 In this study, we have established a new method for scoring of binding pocket residues
323 based on blind docking methodology of highly flexible residue. Knowledge based scoring
324 function, MD simulation and binding free-energy calculations were performed to investigate and
325 validate the binding conformation of Solanesol on Focal adhesion kinase at the molecular level
326 found by LBCSR. This scoring was crucial as blind docking fails to give high confidence data
327 for binding of highly flexible residues.

328

329 Based on the proposed LBCSR score, residues were identified which give high contact
330 score with ligand in multiple blind docking instances. Refined docking was used to identify the
331 best pose for this site. Knowledge based scoring function, DSX, was used to validate the docking
332 result on which 20ns MD simulation was performed. Simulation of only protein structure of
333 FAK protein was performed for establishing a control for MD simulations.

334

335 The MM-PBSA binding free-energy calculations further confirmed the results of the MD
336 simulation. This analysis, established a correlation between the LBCSR and favorably interacting
337 residues. It is in a good agreement with experimental results which shows Solanesol binds at
338 ATP binding site and inhibit the phosphorylation of Focal Adhesion Kinase. This study may help
339 in further analysis and understanding of flexible compounds and inhibition of FAK using the
340 same.

341

342 **Reference**

343 Cohen, L. A., & Guan, J. L. (2005). Mechanisms of focal adhesion kinase regulation.
344 *Current cancer drug targets*, 5(8), 629-643.

345

346 Darden, T., York, D., & Pedersen, L. (1993). Particle mesh Ewald: An $N \cdot \log(N)$ method for
347 Ewald sums in large systems. *The Journal of chemical physics*, 98(12), 10089-10092.

348

349 Frisch, M., Trucks, G.W., Schlegel, H.B., Scuseria, G.E., Robb, M.A., Cheeseman, J.R.,
350 Scalmani, G., Barone, V., Mennucci, B., Petersson, G.A. and Nakatsuji, H., (2009). gaussian
351 09, *Gaussian, Inc*, Wallingford, CT.

352

353 George, D.M., Breinlinger, E.C., Friedman, M., Zhang, Y., Wang, J., Argiriadi, M., Bansal-
354 Pakala, P., Barth, M., Duignan, D.B., Honore, P. and Lang, Q., (2014). Discovery of
355 selective and orally bioavailable protein kinase C θ (PKC θ) inhibitors from a fragment hit.
356 *Journal of medicinal chemistry*, 58(1), 222-236.

357

358 Guan, J. L. (1997). Role of focal adhesion kinase in integrin signaling. *The international*
359 *journal of biochemistry & cell biology*, 29(8), 1085-1096.

360

- 361 Hanahan, D., & Weinberg, R. A. (2011). Hallmarks of cancer: the next generation. *cell*,
362 *144*(5), 646-674.
- 363
- 364 Hanahan, D., & Weinberg, R. A. (2000). The hallmarks of cancer *cell 100*: 57–70.
- 365
- 366 Hetényi, C., & van der Spoel, D. (2002). Efficient docking of peptides to proteins without
367 prior knowledge of the binding site. *Protein science*, *11*(7), 1729-1737.
- 368
- 369 Hetényi, C., & van der Spoel, D. (2006). Blind docking of drug-sized compounds to proteins
370 with up to a thousand residues. *FEBS letters*, *580*(5), 1447-1450.
- 371
- 372 Hess, B., Bekker, H., Berendsen, H. J., & Fraaije, J. G. (1997). LINCS: a linear constraint
373 solver for molecular simulations. *Journal of computational chemistry*, *18*(12), 1463-1472.
- 374
- 375 Hess, B., Kutzner, C., Van Der Spoel, D., & Lindahl, E. (2008). GROMACS 4: algorithms
376 for highly efficient, load-balanced, and scalable molecular simulation. *Journal of chemical
377 theory and computation*, *4*(3), 435-447.
- 378
- 379 Kim, S., Thiessen, P.A., Bolton, E.E., Chen, J., Fu, G., Gindulyte, A., Han, L., He, J., He, S.,
380 Shoemaker, B.A. and Wang, J., 2015. PubChem substance and compound databases. *Nucleic
381 acids research*, gkv951.
- 382
- 383 Kumari, R., Kumar, R., & Lynn, A. (2014). g_mmpbsa□ A GROMACS Tool for High-
384 Throughput MM-PBSA Calculations. *Journal of chemical information and modeling*, *54*(7),
385 1951-1962.
- 386
- 387 Lazebnik, Y. (2010). What are the hallmarks of cancer? *Nature Reviews Cancer*, *10*(4), 232-
388 233.
- 389

390 Massova, I., & Kollman, P. A. (2000). Combined molecular mechanical and continuum
391 solvent approach (MM-PBSA/GBSA) to predict ligand binding. *Perspectives in drug*
392 *discovery and design*, 18(1), 113-135.

393

394 Morris, G. M., Huey, R., Lindstrom, W., Sanner, M. F., Belew, R. K., Goodsell, D. S., &
395 Olson, A. J. (2009). AutoDock4 and AutoDockTools4: Automated docking with selective
396 receptor flexibility. *Journal of computational chemistry*, 30(16), 2785-2791.

397

398 National Center for Biotechnology Information (NCBI). PubChem Compound Database;
399 CID=5477212, <https://pubchem.ncbi.nlm.nih.gov/compound/5477212> (accessed Aug. 11,
400 2016).

401

402 Neudert, G., & Klebe, G. (2011). DSX: a knowledge-based scoring function for the
403 assessment of protein–ligand complexes. *Journal of chemical information and modeling*,
404 51(10), 2731-2745.

405

406 Okamoto, Y., Tsuji, M., & Yamazaki, H. (1994). *U.S. Patent No. 5,306,714*. Washington,
407 DC: U.S. Patent and Trademark Office.

408

409 Pettersen, E. F., Goddard, T. D., Huang, C. C., Couch, G. S., Greenblatt, D. M., Meng, E. C.,
410 & Ferrin, T. E. (2004). UCSF Chimera—a visualization system for exploratory research and
411 analysis. *Journal of computational chemistry*, 25(13), 1605-1612.

412

413 Roe, S. J., Oldfield, M. F., Geach, N., & Baxter, A. (2013). A convergent stereocontrolled
414 synthesis of [3-¹⁴C] solanesol. *Journal of Labelled Compounds and Radiopharmaceuticals*,
415 56(9-10), 485-491.

416

417 Severson, R. F., Ellington, J. J., Schlotzhauer, P. F., Arrendale, R. F., & Schepartz, A. I.
418 (1977). Gas chromatographic method for the determination of free and total solanesol in
419 tobacco. *Journal of chromatography A*, 139(2), 269-282.

420

421 Srivastava, S., Raj, K., Khare, P., Bhaduri, A.P., Chander, R., Raghubir, R., Mahendra, K.,
422 Rao, C.N. and Prabhu, S.K. (2009). Novel hybrid natural products derived from solanesol as
423 wound healing agents. *Indian journal of chemistry. Section B, Organic including medicinal*,
424 *48(2)*, 237.

425

426 Suzuki, H., Tomida, A., & Nishimura, T. (1990). Cytocidal Activity of a Synthetic
427 Isoprenoid, N-Solanesyl-N, N'-bis (3, 4-dimethoxy-benzyl) ethylenediamine, and Its
428 Potentiation of Antitumor Drugs against Multidrug-resistant and Sensitive Cells in vitro.
429 *Japanese journal of cancer research*, *81(3)*, 298-303.

430

431 Tomida, A., & Suzuki, H. (1990). Synergistic Effect in Culture of Bleomycin-group
432 Antibiotics and N-Solanesyl-N, N'-bis (3, 4-dimethoxybenzyl) ethylenediamine, a Synthetic
433 Isoprenoid. *Japanese journal of cancer research*, *81(11)*, 1184-1190.

434

435 Van Aalten, D. M., Bywater, R., Findlay, J. B., Hendlich, M., Hooft, R. W., & Vriend, G.
436 (1996). PRODRG, a program for generating molecular topologies and unique molecular
437 descriptors from coordinates of small molecules. *Journal of computer-aided molecular*
438 *design*, *10(3)*, 255-262.

439

440 Van Nimwegen, M. J., & van de Water, B. (2007). Focal adhesion kinase: a potential target
441 in cancer therapy. *Biochemical pharmacology*, *73(5)*, 597-609.

442

443 Yan, N., Liu, Y., Gong, D., Du, Y., Zhang, H., & Zhang, Z. (2015). Solanesol: a review of its
444 resources, derivatives, bioactivities, medicinal applications, and biosynthesis. *Phytochemistry*
445 *Reviews*, *14(3)*, 403-417.

446

447 Zhao, C. J., Zu, Y. G., Li, C. Y., & Tian, C. Y. (2007). Distribution of solanesol in *Nicotiana*
448 *tabacum*. *Journal of forestry research*, *18(1)*, 69-72.

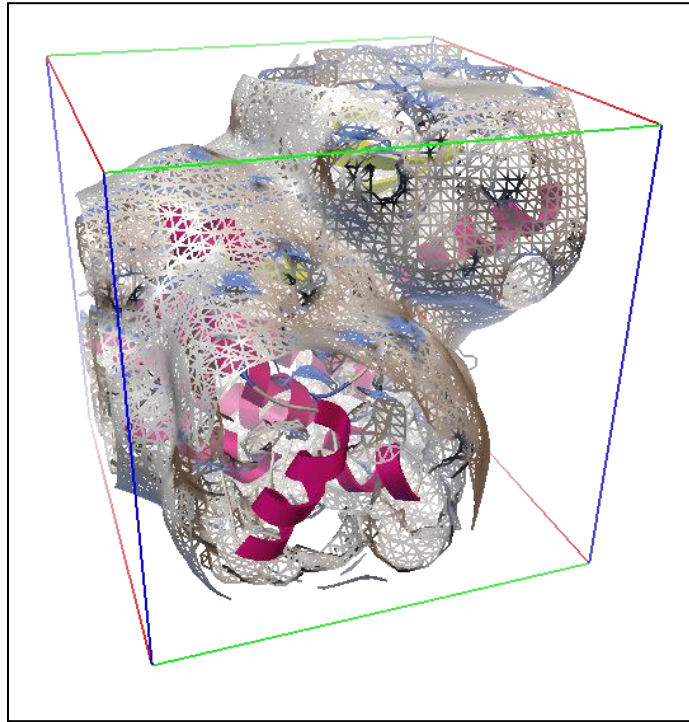
449

450

451

453

455

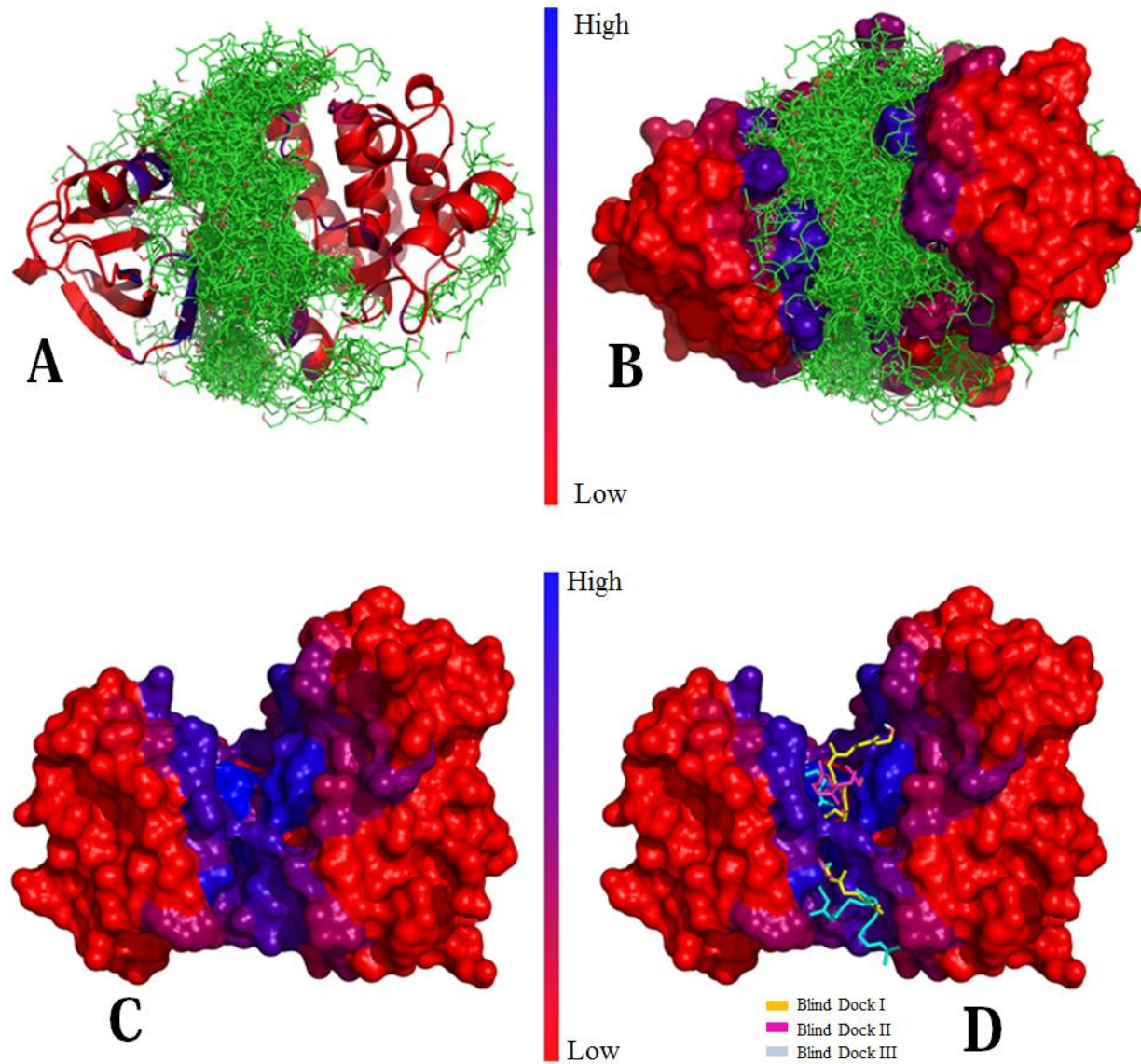


454

455 Figure 1: Autogrid map on Focal adhesion kinase as generated by Autogrid4 when blind docking
456 is done on the whole surface.

457

458



459

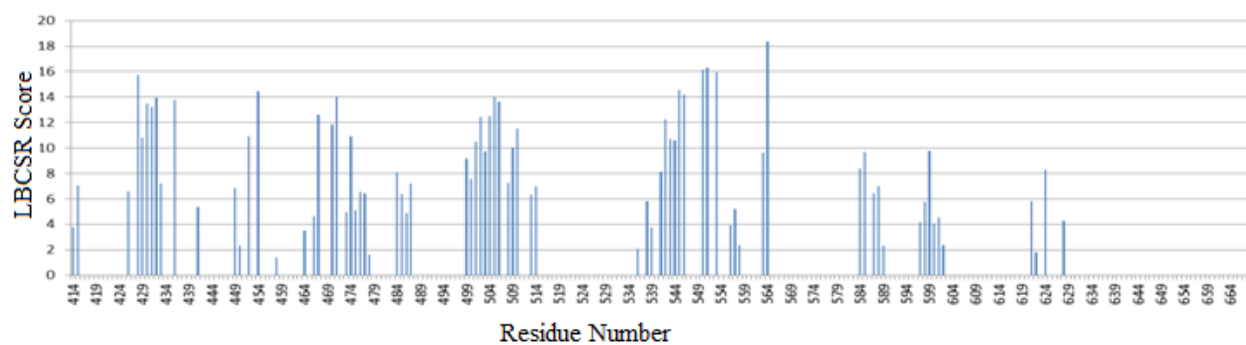
460 Figure 2: (A,B)FAK structure with colour based on LBCSR score show all the conformations
461 docked “blindly”. (C) Only FAK structure with colour based on LBCSR score (B) Best
462 structures (based on binding energy) from the three docking experiments.

463

464

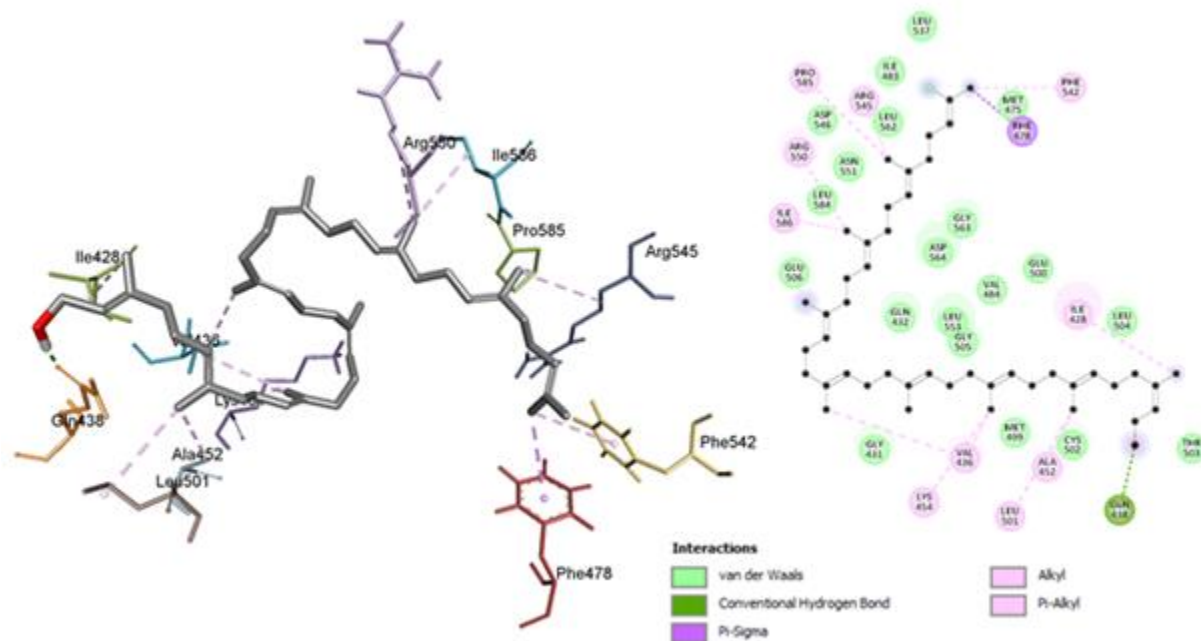
465

466



467
468 Figure 3: Calculated average LBCSR scores for all the residues of Focal Adhesion Kinase for
469 three experiments.

470



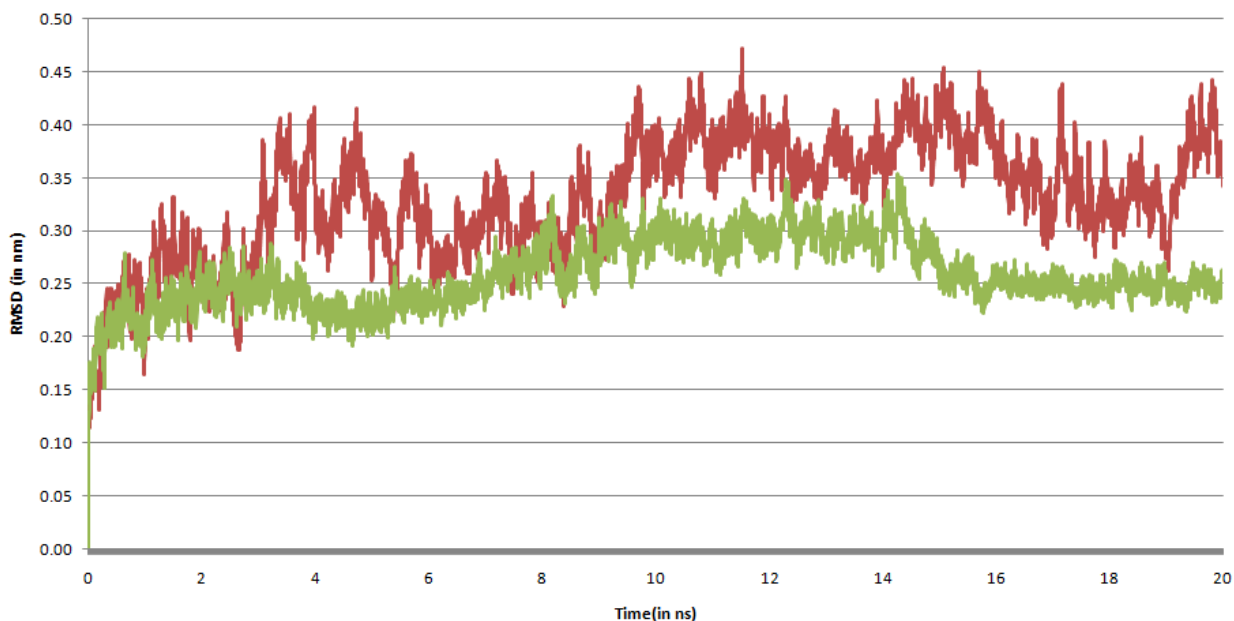
471

472 (A)

(B)

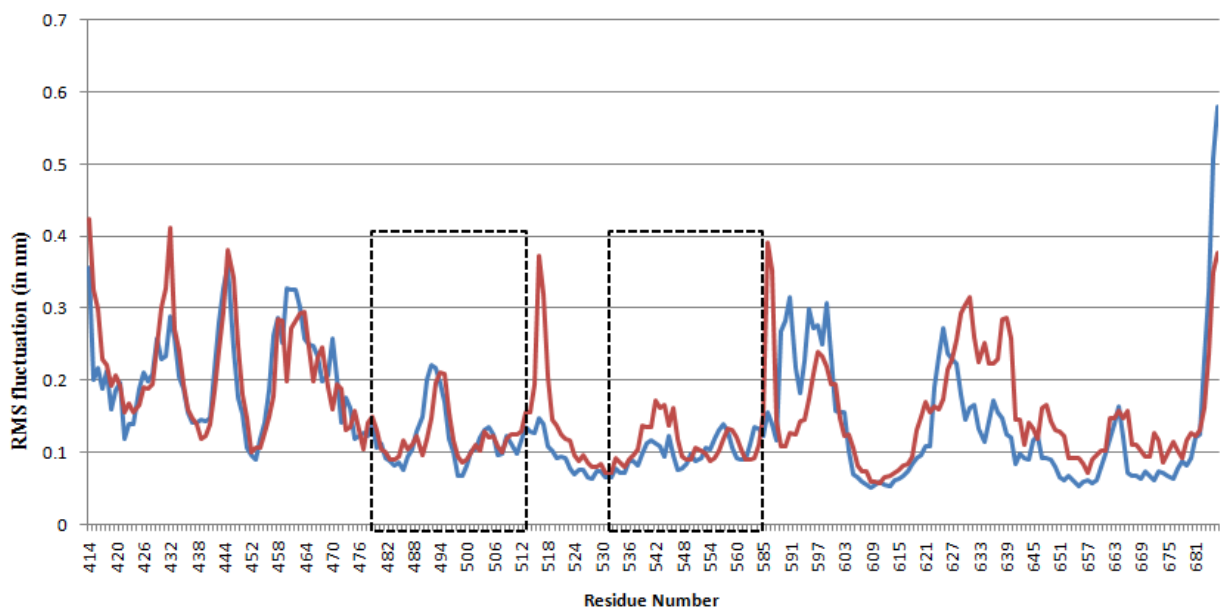
473 Figure 4: 3D (A) and 2D (B) map of Solanesol when bound to Focal Adhesion Kinase (FAK)
474 showing different kinds of interactions.

475



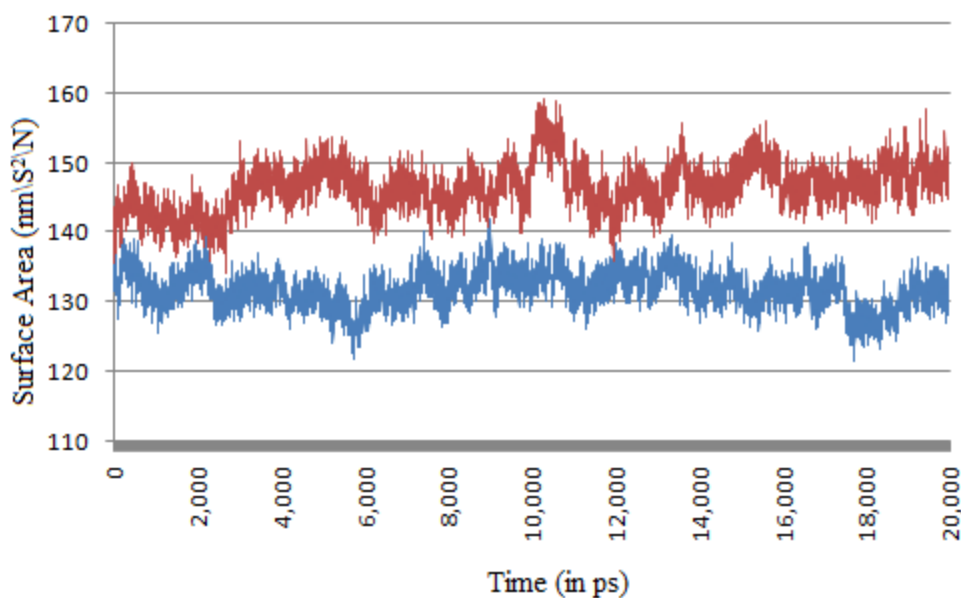
476

477 Figure 5: Root mean square deviation (RMSD) of Focal adhesion kinase backbone atoms when
478 bound to Solanesol. It gets stabilized nearly after 16ns of simulation.



479

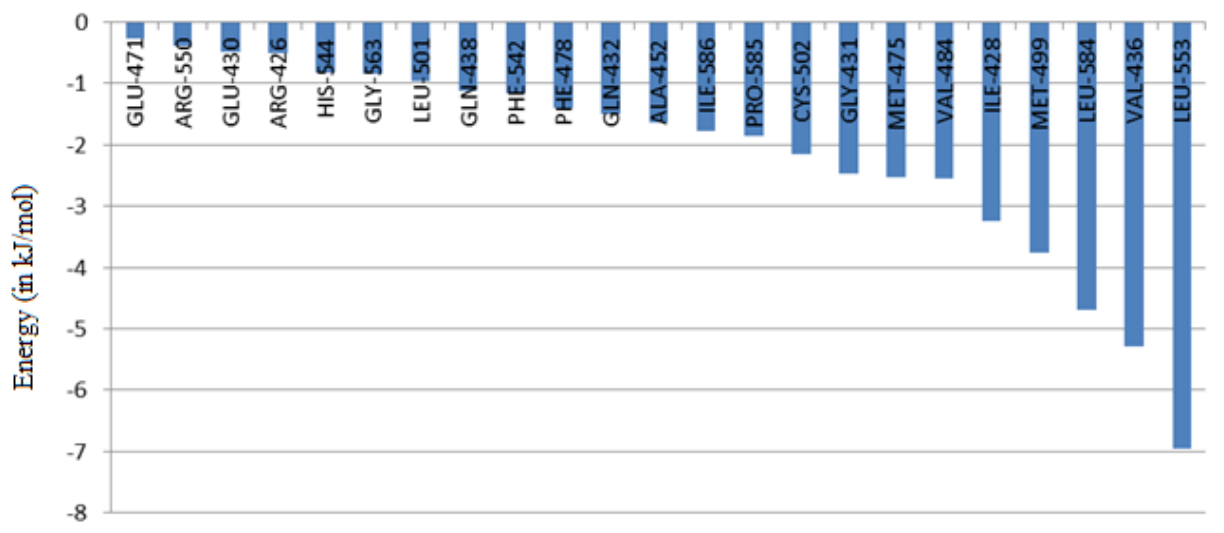
480 Figure 6: RMS Fluctuation (in nm) in alpha carbon atom of each residue in FAK (Red) and
481 Solanesol bound FAK (Blue). Boxes show the binding site region of FAK.



482

483 Figure 7: Total Solvant Accessible Surface Area of Focal Adhesion Kinase with (Blue) and
484 without (Red) bound Solanesol.

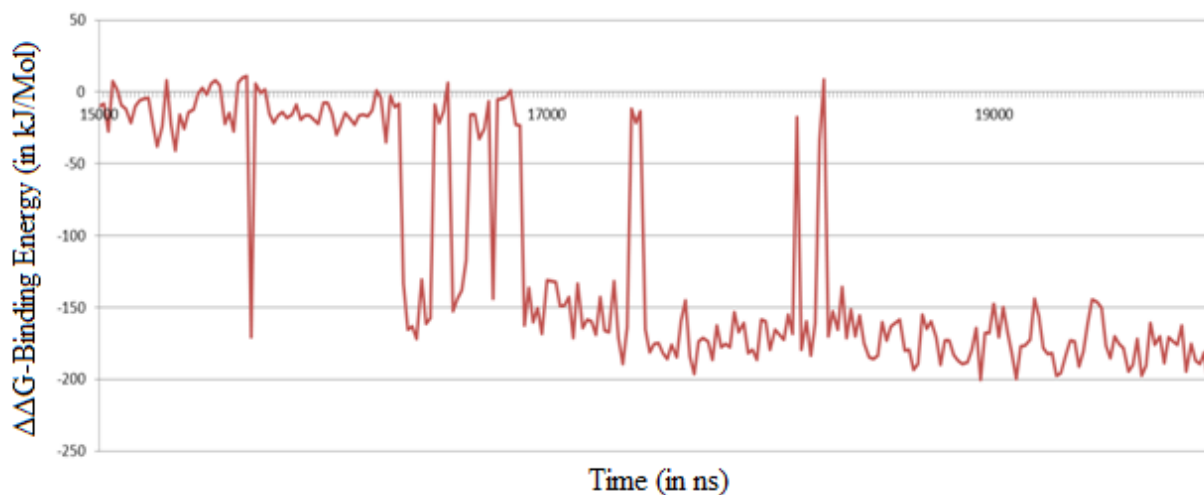
485



486

487 Figure 8: MM-PBSA based residue energy profile for active site residues.

488



489

490 Figure 9: Binding Energy ($\Delta\Delta G$) [kJ/mol] using MM-PBSA method w.r.t time.

491

492

Experiment	Total Conformations	Grid Center	L.B.E (ΔG) in kcal/Mol	Total Cluster	Highest number of member in any cluster	Average B.E of cluster with most number of members
Blind Docking I	500	Center of Protein	-7.08	328	10	0.23
Blind Docking II	200	Center of Protein	-8.54	160	5	-0.19
Blind Docking III	200	Center of Protein	-5.68	187	3	0.13

493 Table 1: Blind docking analysis with three different experiments (with different starting
494 conformations) using standard Autodock protocol

495

496

Residues	Blind Docking I	Blind Docking II	Blind Docking III
LYS-454	5.66	16.50	11.27
ASP-564	8.89	22.35	14.77
ARG-550	7.48	16.33	13.64
GLU-500	2.48	12.06	6.14
ARG-426	3.04	12.11	3.18
GLU-430	5.02	13.87	13.49
LEU-501	4.25	11.98	8.23
GLY-563	4.25	12.08	6.76

GLU-471	6.78	22.50	9.55
GLN-432	5.65	21.14	11.85
ALA-452	4.88	12.30	7.36
CYS-502	5.31	12.32	9.13
PRO-585	4.09	15.50	7.17
HIS-544	4.98	15.97	9.29
GLY-431	5.12	17.82	11.71
VAL-484	3.74	8.93	5.78
MET-475	2.08	10.95	0.69
ILE-428	5.79	16.92	13.77
MET-499	4.42	10.30	5.78
LEU-584	2.30	13.20	10.42
VAL-436	5.55	15.14	11.36
LEU-553	6.30	17.18	13.47

497 Table 2: Top residues with best LBCSR scores of all three experiments

498

	Total Score	Per Contact Score	Torsional Score	SAS Score	Binding Free Energy
Exhaustive Parameter	-166.61	-0.19	-11.13	-16.10	-7.30
Default Parameter	-131.69	-0.17	-12.43	-8.59	-7.25

499 Table 3: DSX, knowledge based scoring of Exhaustive and normal Docking

500

ΔG -vdw (in kJ/Mol)	ΔG -electro (in kJ/Mol)	ΔG -polar (in kJ/Mol)	ΔG -SAS (in kJ/Mol)	$\Delta\Delta G$ -BE (in kJ/Mol)
-145.35	-1.71	52.05	-18.85	-113.85

501 Table 4: MM-PBSA based final Binding free energy of Solanesol with Focal Adhesion Kinase

502

503